The Journal of Experimental Biology 203, 2379–2393 (2000)
Printed in Great Britain © The Company of Biologists Limited 2000
JEB2820

A HYDRODYNAMIC ANALYSIS OF FISH SWIMMING SPEED: WAKE STRUCTURE AND LOCOMOTOR FORCE IN SLOW AND FAST LABRIFORM SWIMMERS

ELIOT G. DRUCKER[1,*] AND GEORGE V. LAUDER[2]

[1]*Department of Ecology and Evolutionary Biology, University of California, Irvine, CA 92697, USA* and
[2]*Museum of Comparative Zoology, Harvard University, 26 Oxford Street, Cambridge, MA 02138, USA*

*e-mail: edrucker@uci.edu

Accepted 11 May; published on WWW 20 July 2000

Summary

Past study of interspecific variation in the swimming speed of fishes has focused on internal physiological mechanisms that may limit the ability of locomotor muscle to generate power. In this paper, we approach the question of why some fishes are able to swim faster than others from a hydrodynamic perspective, using the technique of digital particle image velocimetry which allows measurement of fluid velocity and estimation of wake momentum and mechanical forces for locomotion. We investigate the structure and strength of the wake in three dimensions to determine how hydrodynamic force varies in two species that differ markedly in maximum swimming speed. Black surfperch (*Embiotoca jacksoni*) and bluegill sunfish (*Lepomis macrochirus*) swim at low speeds using their pectoral fins exclusively, and at higher speeds switch to combined pectoral and caudal fin locomotion. *E. jacksoni* can swim twice as fast as similarly sized *L. macrochirus* using the pectoral fins alone. The pectoral fin wake of black surfperch at all speeds consists of two distinct vortex rings linked ventrally. As speed increases from 1.0 to 3.0 $L\,s^{-1}$, where L is total body length, the vortex ring formed on the fin downstroke reorients to direct force increasingly downstream, parallel to the direction of locomotion. The ratio of laterally to downstream-directed force declines from 0.93 to 0.07 as speed increases. In contrast, the sunfish pectoral fin generates a single vortex ring per fin beat at low swimming speeds and a pair of linked vortex rings (with one ring only partially complete and attached to the body) at maximal labriform speeds. Across a biologically relevant range of swimming speeds, bluegill sunfish generate relatively large lateral forces with the paired fins: the ratio of lateral to downstream force remains at or above 1.0 at all speeds. By increasing wake momentum and by orienting this momentum in a direction more favorable for thrust than for lateral force, black surfperch are able to swim at twice the speed of bluegill sunfish using the pectoral fins. In sunfish, without a reorientation of shed vortices, increases in power output of pectoral fin muscle would have little effect on maximum locomotor speed. We present two hypotheses relating locomotor stability, maneuverability and the structure of the vortex wake. First, at low speeds, the large lateral forces exhibited by both species may be necessary for stability. Second, we propose a potential hydrodynamic trade-off between speed and maneuverability that arises as a geometric consequence of the orientation of vortex rings shed by the pectoral fins. Bluegill sunfish may be more maneuverable because of their ability to generate large mediolateral force asymmetries between the left- and right-side fins.

Key words: swimming, pectoral fin locomotion, flow visualization, hydrodynamics, digital particle image velocimetry, black surfperch, *Embiotoca jacksoni*, bluegill sunfish, *Lepomis macrochirus*.

Introduction

What is the physical basis of interspecific variation in the swimming speed of fishes? Virtually all previous work addressing this question has investigated the mechanics of the musculoskeletal system of fishes to determine the limits that muscle physiology imposes on force production and power output. For example, differences among species in swimming speed have been studied from the perspective of recruitment of different muscle fiber types: the contractile properties of red myotomal fibers may dictate the peak power production, and hence maximum locomotor speed, that can be achieved before recruitment of white fibers (Rome et al., 1988, 1992). Similarly, the power output of white muscle fibers has been suggested to limit peak sprint speed (Wardle, 1975; Wardle and Videler, 1979).

While the analysis of internal force and power production is indeed important for understanding variation in fish swimming performance, the mechanical force produced by the swimming musculature must ultimately be transmitted to the water by the body and fin surfaces. The mechanisms by which this transmission is effected also have an important role to play in explaining the limits to fish swimming speed since the fin–water interface is the locus of thrust production.

The major difficulty in undertaking an analysis of force transmission between a swimming fish and the water is that direct measurements of force applied to the aquatic medium have not been possible. In studies of terrestrial locomotion, the use of force plates has allowed quantification of the ground reaction forces experienced by running animals (e.g. Carrier et al., 1998; Roberts et al., 1998), and such direct force measurements have allowed substantial progress in our understanding of the mechanical basis of locomotion on land. For aquatic animals, the application of such devices is precluded by the fluid surroundings in which locomotion occurs. However, in a previous paper (Drucker and Lauder, 1999), we presented an experimental approach to quantifying the forces exerted on the water by freely swimming fishes based on measurement of the fluid momentum added to the wake by the body and fins (see also Wilga and Lauder, 1999; Lauder, 2000).

In the present paper, we address the question of how fishes attain different maximum swimming speeds through a comparative analysis of two species: the bluegill sunfish *Lepomis macrochirus* (family Centrarchidae) and the black surfperch *Embiotoca jacksoni* (family Embiotocidae). The bluegill is a maneuverable planktivore that exhibits slow routine labriform swimming in limnetic habitats (Keast and Webb, 1966; Werner and Hall, 1974). Previous work has shown that adult bluegill have a maximum labriform swimming speed of 1.0 body length s^{-1} and that, above this speed, they switch to combined pectoral and caudal fin propulsion (Gibb et al., 1994; Drucker and Lauder, 1999). Surfperches are common species in near-shore marine habitats of the north Pacific, occurring in kelp forests, rocky reefs and exposed bays of the open coast (DeMartini, 1969; Ebeling et al., 1980). While capable of low-speed maneuvering (Bray and Ebeling, 1975), surfperches also exhibit relatively high-speed locomotion during prey capture and agonistic interactions with congeners (Hixon, 1980; Jensen, 1993). The maximal pectoral-fin swimming speed of adult black surfperch is 2.0 body length s^{-1}, twice that of bluegill sunfish (Fig. 1). Despite their difference in labriform swimming ability, sunfish and surfperch possess very similar pectoral fin morphology and adult body size and shape (see illustrations in Fig. 5).

This paper provides an experimental analysis of the pectoral-fin vortex wake, and associated locomotor forces, in the black surfperch for comparison with data published previously for bluegill sunfish. Our aim is to determine which of several possible hydrodynamic and kinematic variables, acting either singly or in combination, influence the magnitude of the propulsive reaction forces exerted on sunfish and surfperch by the fluid medium. By quantifying wake momentum, vortex jet orientation and fin stroke timing, we present a hydrodynamic interpretation of the observed difference in maximum labriform swimming speed of these slow and fast fishes.

Materials and methods

Fish

Black surfperch (*Embiotoca jacksoni* Agassiz) were netted at Mohawk Reef, Santa Barbara, CA, USA. Animals were housed in a 1300 l salt-water aquarium at an average temperature of 20 °C and fed chopped shrimp twice weekly. Four adult fish of similar size (total body length, L, 20.8±0.3 cm, mean ± S.D.) were selected for study.

Flow visualization

The protocol for inducing steady swimming behavior in the

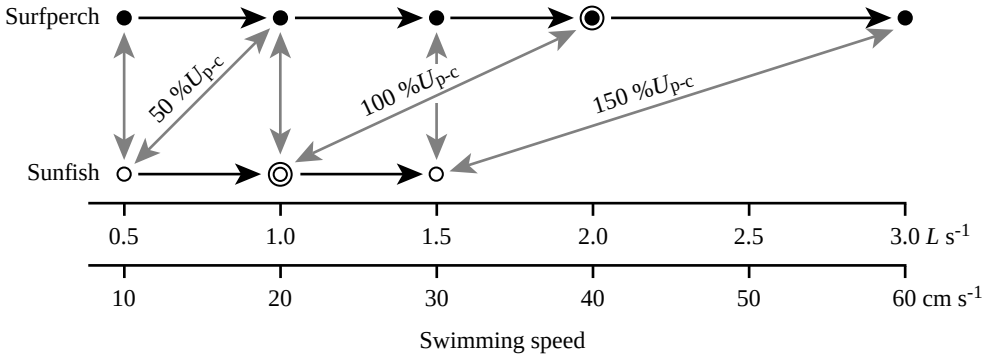

Fig. 1. Conceptual framework used in this paper for intra- and interspecific comparisons of the pectoral fin wake of black surfperch (*Embiotoca jacksoni*) and bluegill sunfish (*Lepomis macrochirus*). The range of swimming speeds examined in each species is indicated by the series of horizontal black arrows. The horizontal axes denote both relative swimming speed, expressed in terms of total body lengths L traveled per second, and corresponding absolute speed (approximate) based on an average L of 20 cm for all fish studied. The effects of swimming speed on wake variables (vortex ring structure, momentum and associated fluid force) are assessed within each species at speeds up to and above the pectoral–caudal gait transition speed U_{p-c} (circled). Note that surfperch of the size studied are capable of swimming at up to 2.0 L s^{-1} with the pectoral fins alone (i.e. before recruitment of axial undulation). This performance limit is twice that of similarly sized sunfish. Interspecific comparisons of wake measurements, indicated by gray arrows, can be made either at individual length-specific or absolute swimming speeds (vertical arrows) or at speeds expressed as a percentage of each species' respective gait transition speed (diagonal arrows). The latter approach provides control for interspecific variation in maximal labriform swimming performance.

black surfperch and for visualizing the vortex wake produced by the pectoral fins closely follows that described for the bluegill sunfish (*Lepomis macrochirus* Rafinesque) studied by Drucker and Lauder (1999). Briefly, individual surfperch swam in the working area (28 cm×28 cm×80 cm) of a recirculating salt water flow tank. Animals swam against low- to medium-speed currents in which propulsion was achieved by oscillation of the paired pectoral fins (0.5, 1.0 and 1.5 $L\,s^{-1}$), at $U_{p\text{-}c}$, the pectoral–caudal gait transition speed (2.0 $L\,s^{-1}$), and at a high speed (3.0 $L\,s^{-1}$) at which the fish required combined pectoral and caudal fin oscillation to hold station (Fig. 1).

A digital particle image velocimetry (DPIV) system was employed that allowed visualization of water flow in planar transections of the pectoral fin wake following the methods that we have used previously (e.g. Drucker and Lauder, 1999; Wilga and Lauder, 1999; see also Lauder, 2000). A 3 W argon-ion laser beam, focused into a thin sheet (1–2 mm thick) and projected into the working area of the flow tank, illuminated reflective microspheres (mean diameter 12 μm) suspended in the water. Two synchronized high-speed video cameras (250 fields s^{-1}, NAC HSV-500) were used to record images of the laser flow field. One camera imaged particles moving within the laser light sheet itself, while the second camera visualized the posterior aspect of the fish by means of a small mirror mounted downstream at 45°. Signals from the two cameras were recorded to videotape as split-screen images, facilitating simultaneous inspection of patterns of fluid flow in the wake and the position of the fish's fin with respect to the laser plane. In separate experiments, the laser was oriented to illuminate flow in the frontal (*XZ*) and parasagittal (*XY*) planes (e.g. Fig. 2). Flow patterns observed in these orthogonal planes were incorporated into a three-dimensional reconstruction of wake geometry.

The experimental portion of this study focuses on visualization of the wake shed by the left pectoral fin of *Embiotoca jacksoni*. Flow patterns are reported for laser planes intersecting the abducted pectoral fin at midspan, the position at which wake vortices were best defined (Drucker and Lauder, 1999). DPIV data were collected from four fish to establish general wake flow patterns and vortex dynamics. Forty-two pectoral fin strokes performed by two of these individuals were subjected to detailed quantitative analysis. In total, 105 video image pairs were selected from these fin beats to determine planar flow patterns in the wake of *E. jacksoni* during labriform locomotion.

Image analysis and wake measurements

Digitized video images of the pectoral fin wake of *Embiotoca jacksoni* were evaluated using a DPIV cross-correlation algorithm (Insight v. 3.0 software, TSI Inc., St Paul, MN, USA) to yield two-dimensional flow fields consisting of 400 uniformly distributed water velocity vectors (Raffel et al., 1998). Post-processing of DPIV data was performed according to Drucker and Lauder (1999). From each validated velocity vector, the average free-stream water velocity was subtracted to reveal vortical flow structures. Several variables describing the planar geometry of the vortex wake were then measured. (i) Momentum angle ψ was measured between the upstream–downstream axis of flow and the axis traversing the paired centers of counterrotating vortices (see Fig. 4 for an illustration of angle and Figs 2, 3 for the location of vortices relative to fish's body). The angle ψ reflects the degree to which vortex rings introduced into the downstream wake are tilted relative to the orientation of upstream incident flow. (ii) Jet angle ϕ was the average angle of inclination of velocity vectors comprising the central region of jet flow between paired vortices of opposite-sign rotation (see Fig. 6). Since the central jet flow produced by a pectoral fin may not be precisely perpendicular to the vortex ring plane (Drucker and Lauder, 1999), it was necessary to measure ψ and ϕ independently. Both angles were measured separately for vortices shed during fin downstroke and upstroke. (iii) Vorticity components were calculated (see Drucker and Lauder, 1999) and plotted for the frontal and parasagittal planes to highlight centers of fluid rotation.

Locomotor forces experienced by the pectoral fins of the surfperch were calculated as the reaction to the rate of change of the wake's momentum over time (Ellington, 1984; Drucker and Lauder, 1999). The time-averaged total fluid force ($\bar{F}$) generated during the pectoral fin stroke was calculated from Milne-Thomson (1966) as:

$$\bar{F} = M/T, \tag{1}$$

where, in the present application, M is the momentum of a vortex ring shed into the wake and T is the duration of pectoral fin movement. Vortex ring momentum was determined separately at the end of the downstroke and at the end of the upstroke as the product of seawater density (1023 kg m^{-3} at 20 °C), the mean circulation magnitude of paired vortices in midline sections of the ring and the projected area of the vortex ring onto the plane of analysis (see equation 3 in Drucker and Lauder, 1999). In calculations of fluid force developed during each fin half-stroke, T was taken separately as the duration of fin downstroke and fin upstroke.

Within the frontal plane of analysis, the force exerted by the left pectoral fin was geometrically resolved into two perpendicular components according to the average orientation of the central fluid jet (i.e. mean ϕ). For each fin beat analyzed, the total force arising in reaction to the wake of the left pectoral fin was partitioned into a thrust component parallel to the X axis and a non-propulsive medially oriented component parallel to the Z axis (see Fig. 2). From the parasagittal plane of analysis, the lift forces exerted on the fish were calculated by resolving geometrically the orientation of the central fluid jet into downstream (thrust) and vertical components parallel to the X and Y axes, respectively. To obtain estimates of the total reaction force experienced by the entire animal during each fin stroke cycle, forces calculated for the left pectoral fin were doubled to account for the simultaneous action of the contralateral fin (Drucker and Lauder, 1999).

Interspecific comparisons

The black surfperch studied in this paper exhibit an average maximum labriform swimming speed, expressed in body lengths traveled per second, that is twice that of the bluegill sunfish described by Drucker and Lauder (1999). As a result, differences in animal activity level at individual body-length-specific swimming speeds can confound interspecific comparisons of wake morphology and dynamics. To control for differences in labriform swimming performance, cross-taxonomic wake comparisons are made at swimming speeds expressed as fixed percentages of each species' respective pectoral–caudal gait transition speed $U_{p\text{-}c}$ (Drucker, 1996). Since hydrodynamic forces are directly related to the absolute speed of propulsion, however, Fig. 1 is provided to allow translation of speeds expressed in terms of $\%U_{p\text{-}c}$ to $cm\,s^{-1}$. The surfperch and sunfish compared in this paper are not significantly different in total body length (*t*-test, d.f.=10, P=0.33; pooled mean ± S.D.=20.4±0.8 cm, N=4 and 8, respectively) and therefore comparisons at given length-specific speeds may equivalently be considered as absolute speed comparisons.

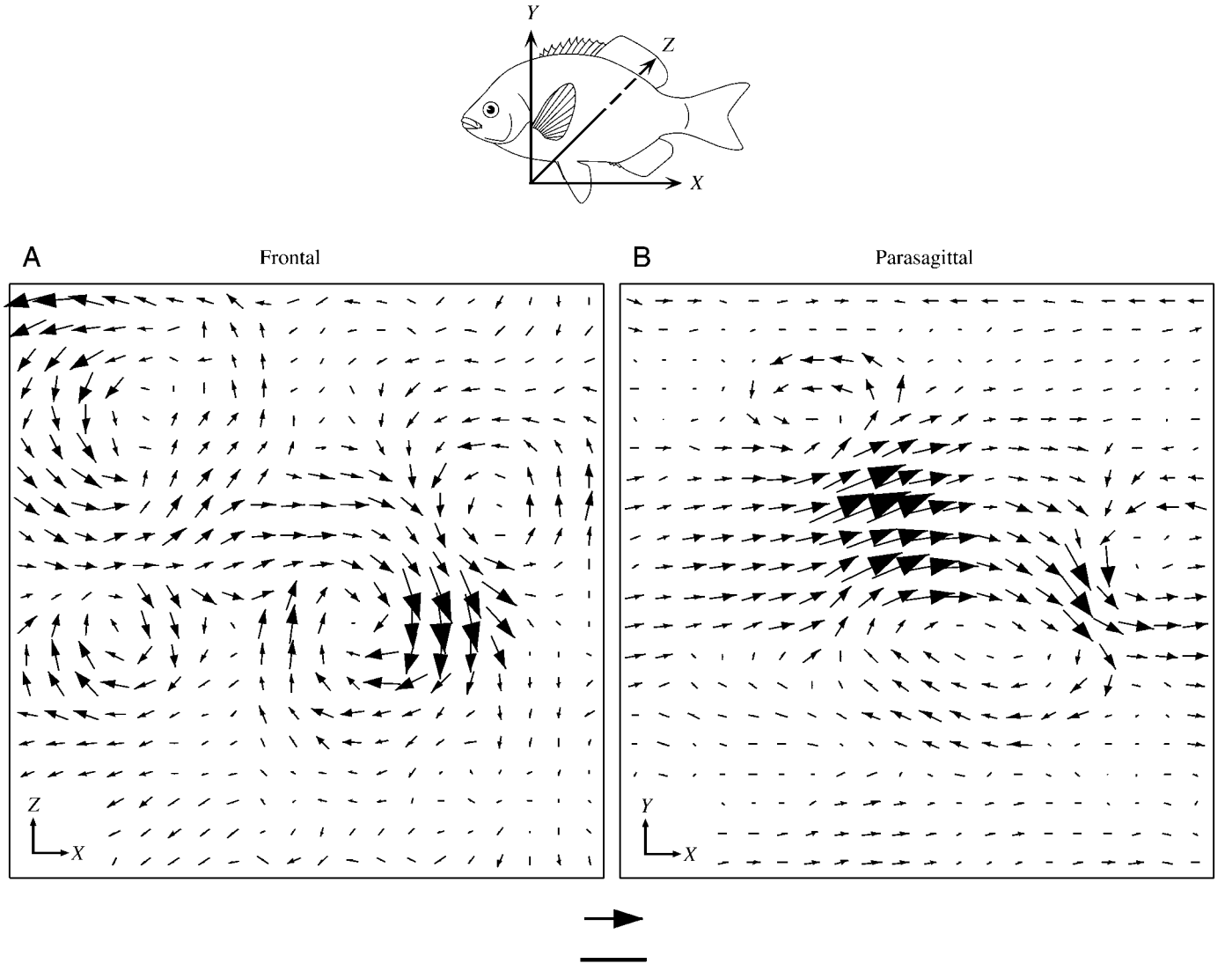

Fig. 2. Water velocity vector fields in perpendicular planar transections of the pectoral fin wake of the black surfperch during single strides of labriform swimming at $1.0\,L\,s^{-1}$. Flow patterns are shown at the end of fin upstroke and illustrate the general patterns of vortex wake morphology observed at all speeds (cf. Fig. 3). In the frontal plane (*XZ*), four discrete vortices are observed: the right-hand pair of counterrotating vortices is created during the fin downstroke, and the left-hand pair is formed on the upstroke. In the parasagittal plane (*XY*), three vortices are visible. The right-hand pair appears on the downstroke, with the largest and most ventral vortex strengthened during the fin rotation at stroke reversal. The single vortex in the upper left develops during the upstroke. Note that the axes at the top of the figure define the perpendicular orientations of the two flow planes, but that the planes illustrated in this paper intersect the abducted left pectoral fin at midspan (see Fig. 2 in Drucker and Lauder, 1999). A mean horizontal flow speed of $1.0\,L\,s^{-1}$ ($21\,cm\,s^{-1}$) from left to right has been subtracted from each velocity vector to reveal the vortices. Scales: arrow, $10\,cm\,s^{-1}$; bar, 1 cm. *L*, total body length.

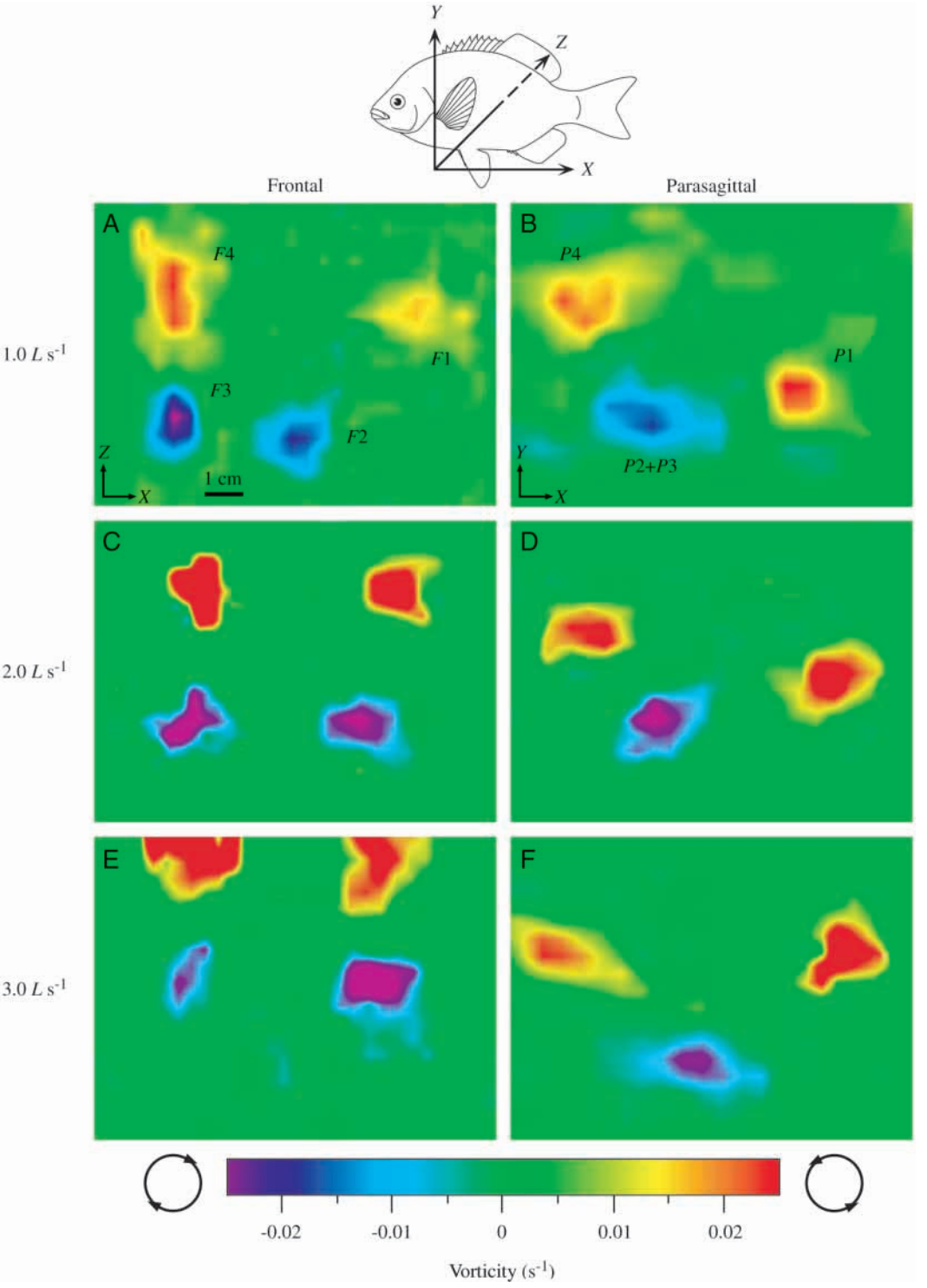

Fig. 3. Vorticity components for horizontal (frontal, *XZ*) and vertical (parasagittal, *XY*) planes in the pectoral fin wake of the black surfperch. Representative patterns of fluid rotation are shown for single fin beats at speeds representing 50, 100 and 150 % of the pectoral–caudal gait transition speed (cf. Fig. 1). The degree of rotation (vorticity) is represented by pseudocolors; the direction of rotation is indicated by icons at either end of the vorticity color scale. The gross morphology of flow in each perpendicular plane remains constant across speed. However, the downstroke vortex pair observed in the frontal plane (*F*1, *F*2) shows a progressive downstream reorientation, and the triple vortex grouping in the parasagittal plane as a whole undergoes counterclockwise rotation. Vortices observed in the frontal plane (*F*1, *F*2, *F*3 and *F*4) are named in order of appearance during the fin beat cycle (i.e. downstroke starting, downstroke stopping, upstroke starting and upstroke stopping vortices, respectively). Similar abbreviations are used for vortices detected in the parasagittal plane: *P*1–*P*4. *P*2+*P*3 is the combined downstroke stopping–upstroke starting vortex. See Drucker and Lauder (1999) for a discussion of the dynamics of vortex generation. *L*, total body length. Scale bar applies to A–F.

Results

Vortex flow patterns

Surfperch

As seen in perpendicular planar transections, the wake of the pectoral fin in black surfperch consists of arrays of well-developed, counterrotating vortices. An example of perpendicular velocity flow fields calculated from video images of particle movement during steady labriform swimming is given in Fig. 2. Four vortices are observed in the frontal plane, two produced during the downstroke of the fin, and two produced during the upstroke. In the parasagittal plane, three vortices are visible at the end of the fin stroke cycle. The first vortex to appear in this vertical plane arises during early downstroke, the final vortex is produced by the upstroke and a third vortex is created in the intermediate period of fin rotation during the transition from downstroke to upstroke. In all cases, between paired vortices of opposite-sign rotation flows a jet of fluid oriented approximately perpendicular to the longitudinal axis traversing both vortex centers.

The gross morphology of the wake in planar sections remains constant over the entire range of swimming speeds examined in *Embiotoca jacksoni*: the wake at all speeds consists of four centers of vorticity in the frontal plane and three in the parasagittal plane (Fig. 3). However, the relative positions of wake vortices within each plane do change as speed increases. In the frontal plane, the downstroke vortices (Fig. 3A, *F*1, *F*2) undergo a progressive reorientation with speed, describing an increasing momentum angle with respect to the *X* axis (ψ_D in Fig. 4A). At the highest swimming speed studied ($3.0\,L\,s^{-1}$, Fig. 3E), the downstroke vortices in the frontal plane fall along an axis perpendicular to the longitudinal body axis of the fish (ψ_D is approximately 90 °; see Fig. 4A), reflecting a primarily downstream-oriented momentum flow. The upstroke vortex pair (Fig. 3A, *F*3, *F*4) changes little in orientation with increasing speed (ψ_U ranges from 79 to 90 °, Fig. 4A). In the parasagittal plane, the downstroke starting vortex (Fig. 3B, *P*1) and the combined downstroke stopping–upstroke starting vortex (*P*2+*P*3) define a steadily increasing momentum angle with respect to the *X* axis above $1.0\,L\,s^{-1}$ (Fig. 4B, ψ_D). A similar pattern is observed for *P*2+*P*3 and the upstroke stopping vortex *P*4 (Figs 3B, 4B: ψ_U).

A three-dimensional interpretation of the wake structure for the surfperch at three speeds is shown in Fig. 5A–C. The reconstruction is based upon the numbers and relative positions of discrete centers of vorticity seen in perpendicular flow planes (Fig. 3) and the average momentum angles of downstroke and upstroke vortex pairs (Fig. 4). Like the bluegill sunfish studied previously (Drucker and Lauder, 1999), the black surfperch sheds vortex rings into the wake during labriform swimming. Across the entire range of swimming speeds studied, the pectoral fin wake takes the form of paired vortex rings that are linked ventrally (as demonstrated by *P*2+*P*3 observed in the parasagittal plane). With increasing speed, the similar rate of increase in ψ for the downstroke and upstroke in the parasagittal plane (Fig. 3B,D,F; Fig. 4B, $1.0–3.0\,L\,s^{-1}$) indicates a counterclockwise rotation of the entire linked-pair vortex ring structure, as viewed from a lateral perspective.

Interspecific comparison

The wake morphology of the bluegill sunfish differs markedly from that of the black surfperch. The vortex ring structures for *Lepomis macrochirus* shown in Fig. 5D–F are based on patterns of vorticity observed in frontal- and parasagittal-plane flow fields (see Figs 4, 6 in Drucker and Lauder, 1999) and mean momentum angles of vortex pairs (Fig. 4C,D). At 50 % of the pectoral–caudal gait transition speed $U_{p\text{-}c}$, sunfish produce a single vortex ring per stride with each pectoral fin (Fig. 5D), as opposed to the linked pair of rings produced by surfperch (Fig. 5A). At higher speeds, the sunfish upstroke becomes hydrodynamically active, shedding a second vortex filament that is proposed to terminate on the fish's body rather than forming a complete loop. The partial upstroke vortex ring in *L. macrochirus* is linked to the downstroke ring laterally (Fig. 5E) and, at the highest speed, ventrally (Fig. 5F). At and above $U_{p\text{-}c}$, both species exhibit large differences in the mean momentum angle measured in the parasagittal plane for downstroke and upstroke vortex pairs (Fig. 4B,D). In sunfish, as in surfperch, the ring planes are tilted (i.e. rotated away from each other around the fish's mediolateral axis), but in general the sunfish's rings are more upright, reflecting a relatively small component of velocity oriented along the vertical (dorsoventral) axis of the fish in the central fluid jet of each ring (cf. Fig. 5C,F).

A further interspecific difference in wake morphology relates to the orientation of the fluid jet induced by each pair of counterrotating vortices in the frontal plane of analysis. With increasing swimming speed, the momentum angle of the downstroke vortex pair (ψ_D) measured in the frontal plane decreases sharply in sunfish (Fig. 4C) because the plane of the downstroke vortex ring rotates laterally (Fig. 5D–F, see vortices *F*1 and *F*2). The opposite trend is observed for the surfperch: ψ_D becomes maximal at the highest swimming speed (Fig. 4A) and the downstroke ring faces increasingly downstream (Fig. 5A–C, *F*1, *F*2). Corresponding to this difference in the speed-dependence of ψ is interspecific variation in the central jet angle ϕ. Mean jet angles for the downstroke vortex ring (ϕ_D) in the frontal plane are shown in Fig. 6. For the surfperch, mean ϕ_D decreases from 55 to nearly 0 ° at speeds between 50 and 150 %$U_{p\text{-}c}$ ($1.0–3.0\,L\,s^{-1}$). In contrast, the mean jet angle for sunfish increases from 55 to 86 ° over the comparable range of swimming speeds ($0.5–1.5\,L\,s^{-1}$). Unlike the downstroke jet angle, ϕ for the upstroke shows little variation with speed in the frontal plane for surfperch (pooled mean across speeds -3.2 ± 1.3 °, N=8, mean ± S.E.M.), and the momentum flow remains directed largely downstream. The absence of paired frontal-plane vortices on the upstroke of sunfish (Fig. 5D–F) precluded

measurement of corresponding upstroke jet angles for this species.

In both sunfish and surfperch, independent measurements of vortex ring radius R from perpendicular wake planes exhibited only minor variation. Vortex rings of sunfish showed no significant differences in R measured in the frontal and parasagittal planes of analysis at each of the three swimming speeds studied (unpaired t-tests, d.f.=9–12, P=0.08–0.29). In surfperch, the ring radii were significantly greater (P<0.05) in the parasagittal plane than in the frontal plane at all speeds, but the absolute variation in ring dimensions was small: estimates of R differed by only 0.07–0.26 cm, or 2–8 % of mean ring diameter, in the two planes. Accordingly, ring radii for both species were pooled across the two planes (Table 1), and a circular configuration of vortex rings was assumed for calculations of wake momentum and locomotor force.

Locomotor forces

The mean force arising in reaction to the pectoral fin wake may be estimated from both the timing of the fin stroke and the momentum of shed vortices (equation 1). These variables are plotted separately against swimming speed in Fig. 7. At swimming speeds representing comparable levels of activity, surfperch and sunfish show no significant differences in the duration of the downstroke (Fig. 7A) or upstroke, except at the pectoral–caudal gait transition speed (Fig. 7B). At $U_{p\text{-}c}$, the black surfperch completes the upstroke an average of 55 ms faster than the bluegill sunfish, a difference representing 15 % of the period of propulsive fin movements. Unlike the timing of fin half-strokes, wake momentum varies markedly between the species. At all speeds examined, the vortex rings shed by surfperch carry significantly more momentum into the wake than those of sunfish (Fig. 7C). Correspondingly, time-averaged thrust produced by the pectoral fins of surfperch exceeds that of sunfish at the same percentages of $U_{p\text{-}c}$ (Fig. 7D) (unpaired t-tests at 50, 100 and 150 %$U_{p\text{-}c}$, d.f.=7–9, P<0.001). When swimming at the same length-specific speeds (0.5, 1.0 and 1.5 $L\,s^{-1}$, Fig. 1), the two species show a similar difference in thrust production (unpaired t-tests, d.f.=6–9, P<0.05).

In both species, the total thrust produced by the left and right fins together increases linearly up to $U_{p\text{-}c}$ and plateaus above this speed (Fig. 7D). For the purpose of comparing the rate of increase in thrust with speed in the two species, least-squares linear regressions were performed. To determine regression coefficients for the range of data plotted up to $U_{p\text{-}c}$ only, regression lines were not forced through the origin. In the region of linear increase in stride-specific thrust (25–100 %$U_{p\text{-}c}$ for *E. jacksoni*; 50–100 %$U_{p\text{-}c}$ for *L. macrochirus*, Fig. 7D), regression coefficients showed a significant difference from zero in each species (P<0.001), but no significant interspecific difference. The slope of the regression line was 0.063±0.012 N per $L\,s^{-1}$ for the surfperch and 0.060±0.014 N per $L\,s^{-1}$ for the sunfish (means ± S.E.M.).

From frontal-plane flow fields, a downstream-oriented force, whose reaction is propulsive, and a non-propulsive laterally oriented force exerted on the fluid were calculated for each fin stroke. The relative magnitude of these two perpendicular components of locomotor force varies significantly between species. In the surfperch, the ratio of force directed laterally *versus* downstream declines sharply with speed, reaching 0.07 (or roughly 1:10) on average at the maximum speed examined,

Table 1. *Vortex ring measurements related to wake momentum for black surfperch and bluegill sunfish*

		Surfperch		Sunfish	
Swimming speed	Stroke	Ring radius × 10^2 (m)	Circulation × 10^4 ($m^2\,s^{-1}$)	Ring radius × 10^2 (m)	Circulation × 10^4 ($m^2\,s^{-1}$)
0.5 $L\,s^{-1}$	D	1.87±0.26	21.6±2.0	1.79±0.07	51.7±6.3
	U	1.99±0.15	24.3±3.0	–	–
1.0 $L\,s^{-1}$	D	2.67±0.24	28.5±4.0	1.55±0.10	24.3±2.1
	U	2.19±0.14	31.0±3.5	1.71±0.14	28.4±1.7
1.5 $L\,s^{-1}$	D	3.21±0.35	26.5±2.2	1.54±0.08	20.9±2.3
	U	1.55±0.21	29.2±2.9	1.24±0.13	21.9±3.7
2.0 $L\,s^{-1}$	D	3.17±0.38	38.4±5.3	–	–
	U	1.76±0.11	42.2±3.0		
3.0 $L\,s^{-1}$	D	2.58±0.33	36.6±3.4	–	–
	U	1.84±0.10	49.2±5.3		

Data are given for the end of each half-stroke as means ± S.E.M. At each speed, N=3–14 pectoral fin strokes performed by two individuals of each species.

All measurements are reported as averages across the frontal and parasagittal planes of analysis (see text) except for the upstroke vortex ring of the sunfish, for which only parasagittal-plane data were available (see Fig. 5E,F). For each plane, circulation was measured as the average magnitude of values for paired clockwise and counterclockwise vortices.

Data for sunfish are from Drucker and Lauder (1999).

D, downstroke; U, upstroke; L, total body length.

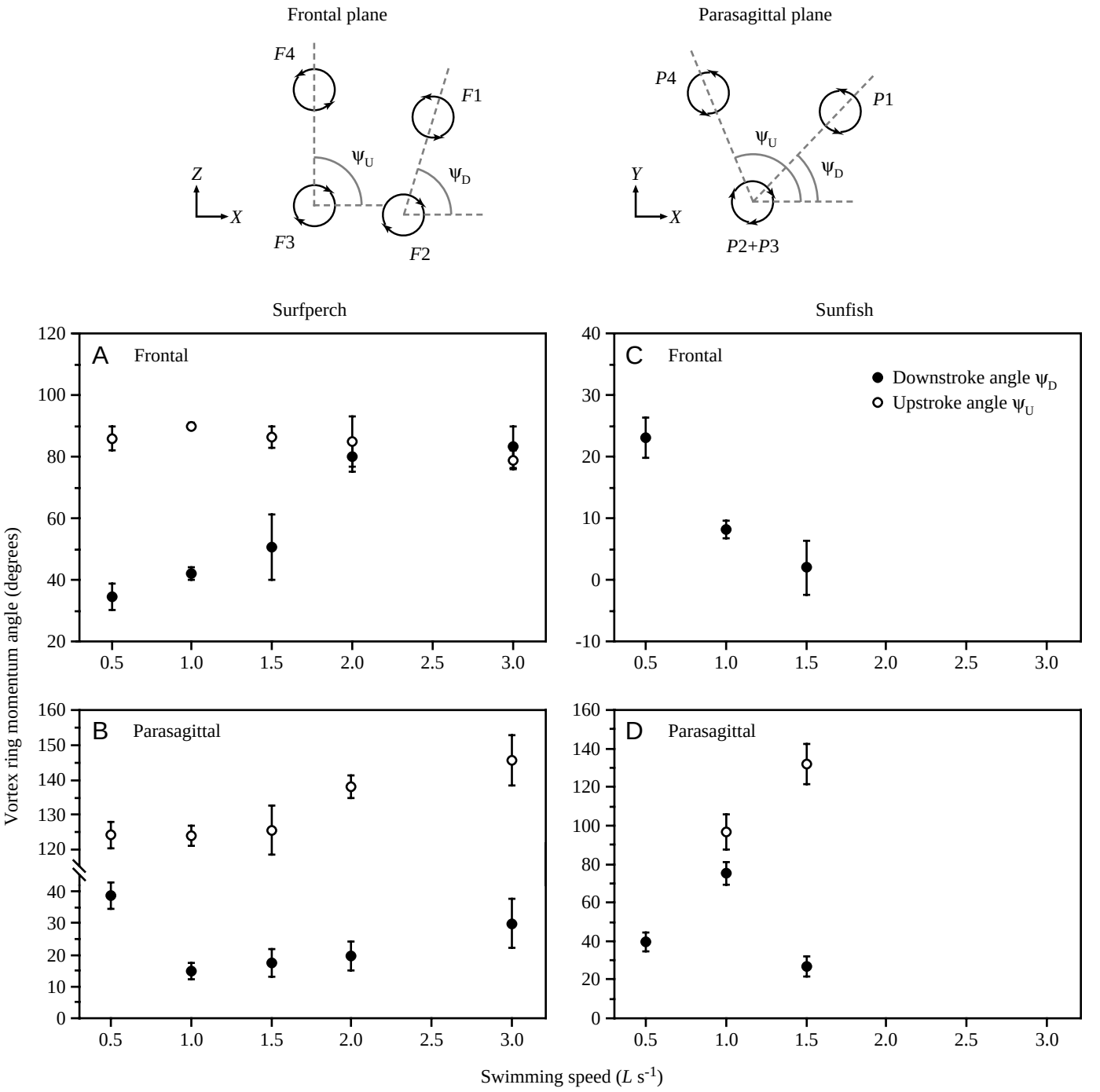

Fig. 4. Relationship between vortex ring momentum angle and swimming speed for surfperch and sunfish. Plotted values are means ± S.E.M. (N=3–6 fin strokes). Momentum angle, defined graphically at the top of the figure, was measured separately for the downstroke (ψ_D) and upstroke (ψ_U) in each of the two perpendicular planes. X–Y–Z axes are provided to aid orientation of angles with respect to the fish and its vortex wake (cf. Figs 2, 3). Note that, in the parasagittal plane, the center of combined vortex $P2$+$P3$ served as the vertex of both measured angles. The wake structure of the sunfish precluded measurement of ψ_U in the frontal plane and at $0.5\,L\,s^{-1}$ in the parasagittal plane. In three-dimensional reconstructions of the wake (Fig. 5), ψ_D and ψ_U are represented by the degree to which the downstroke and upstroke vortex rings are tilted in space. L, total body length. Other abbreviations are as in Fig. 3. Sunfish data are from Drucker and Lauder (1999).

150 %$U_{p\text{-}c}$ (Fig. 8). In the sunfish, in contrast, this ratio remains at approximately 1 (mean 1.25–1.02) over the range of swimming speeds studied. Thus, at 150 %$U_{p\text{-}c}$, the bluegill sunfish exerts forces of comparable magnitude sideways and backwards with each pectoral fin during the stroke period (Fig. 8).

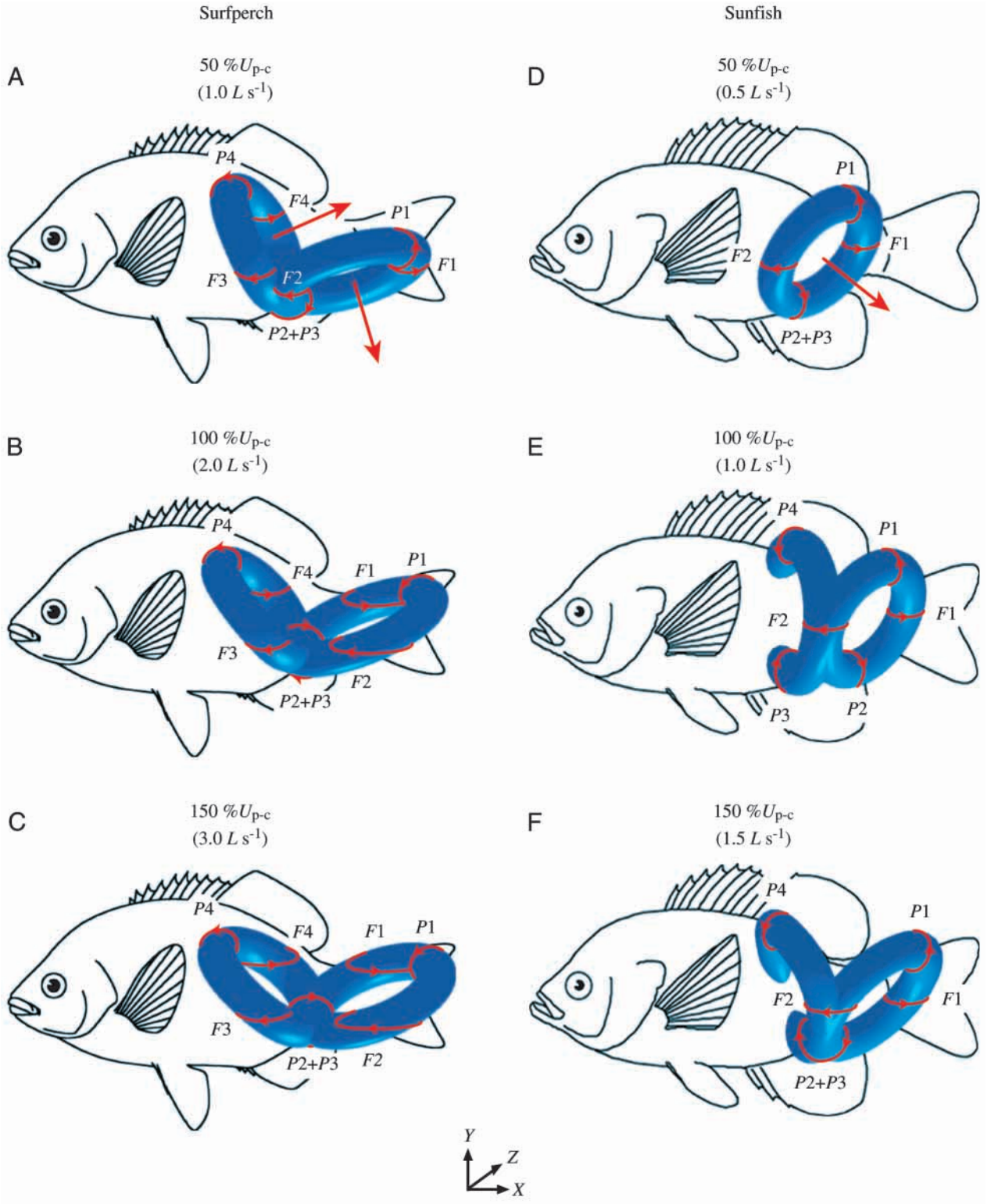

Fig. 5. Schematic three-dimensional representation of the pectoral fin wake at the end of the upstroke in the black surfperch (A–C) and bluegill sunfish (D–F). Vortex rings were reconstructed from the geometry of vortex pairs observed in perpendicular planar transections of the wake (surfperch, Figs 3, 4; sunfish, Drucker and Lauder, 1999). Curved arrows represent centers of vorticity visualized using digital particle image velocimetry. Straight arrows indicate the direction of jet flow through the center of each vortex ring. For simplicity, jets are represented only at 50 %U_{p-c}, but in fact are present at all speeds, oriented approximately normal to each ring plane. Variation in wake structure among swimming speeds and between species is proposed to reflect differences in the magnitude of locomotor force developed (see text for discussion). U_{p-c}, pectoral–caudal gait transition speed; L, total body length. Other abbreviations are as in Fig. 3.

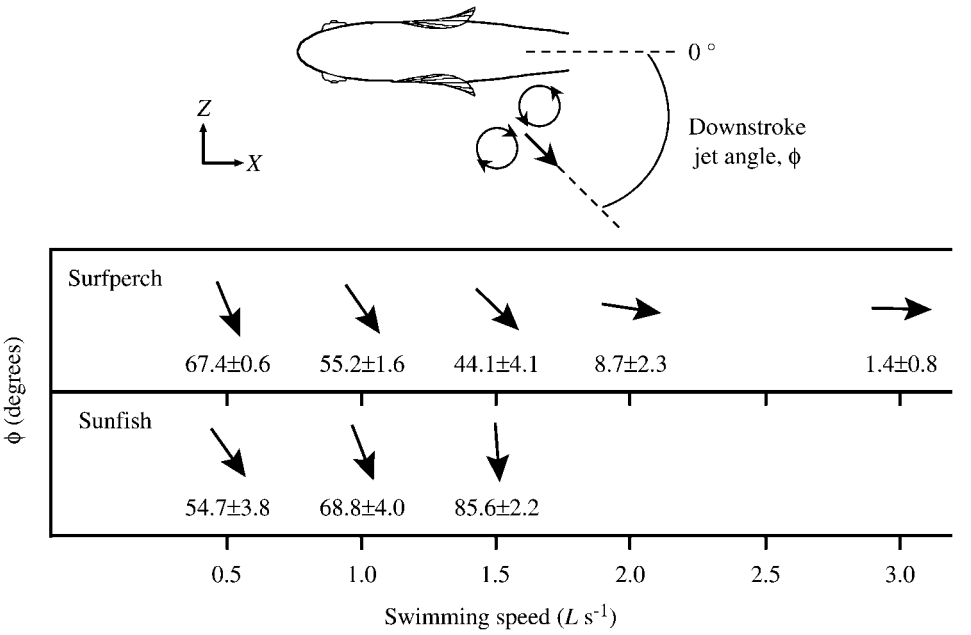

Fig. 6. Orientation of jet flow associated with the downstroke vortex ring plotted as a function of swimming speed in the black surfperch and bluegill sunfish. The jet angle ϕ measured in the frontal plane (*XZ*) is defined as 0 ° when velocity vectors comprising the jet are oriented on average directly downstream and as 90 ° when oriented laterally (see illustration at the top of the figure). For both species, mean downstroke ϕ is represented by the orientation of the thick arrows (accompanying values are means ± S.E.M., *N*=3–8 fin strokes). With increasing swimming speed, the faster fish (surfperch) directs the downstroke jet increasingly downstream, while the slower fish (sunfish) progressively reorients the jet laterally. Sunfish data at 0.5 $L\,s^{-1}$ are from Drucker and Lauder (1999). *L*, total body length.

Discussion

Pectoral-fin wake structure

Although differing twofold in maximum labriform swimming speed, the fishes examined in this study exert mechanical force on their fluid surroundings by means of a similar strategy: the production of momentum-bearing vortex rings (Fig. 5). It is important to emphasize that the formation of such biological wake structures is not directly analogous to that of man-made vortex flows of the same shape. It is incorrect to assume that the paired vortices generated by the fish's fin are merely a byproduct of the central fluid jet, as is the case, for instance, for vortices generated by fluid ejected from nozzles (e.g. Maxworthy, 1972). The leading- and trailing-edge vortices produced by the flexible, oscillating pectoral fin on each half-stroke arise concurrently with, rather than as a consequence of, the central jet (see Fig. 3 in Drucker and Lauder, 1999). Therefore, the entire vortex ring (i.e. vortex filament+central jet) – the visible record of momentum transfer within the wake – is considered in evaluating mechanisms of propulsion.

The vortex ring wake of the pectoral fin is a finding in agreement with the general wake structure observed in other animals moving with paired appendages through fluid (Spedding et al., 1984; Rayner et al., 1986; Spedding, 1986; Brodsky, 1991; Dickinson, 1996). Morphological features of the reconstructed pectoral fin wake, however, differ substantially in *Lepomis macrochirus* and *Embiotoca jacksoni*. Such interspecific variation in wake structure can be understood in terms of differing demands for locomotor force.

The most pronounced difference in the form of the wake is seen at speeds below the pectoral–caudal gait transition speed. At 50 %$U_{p\text{-}c}$, the sunfish generates a single vortex ring per stroke period (Fig. 5D), a structure developed during the fin downstroke and the fin rotation at stroke reversal. The slow, and relatively weak, upstroke at this low swimming speed results in no detectable circulation in the wake (Drucker and Lauder, 1999). The surfperch at this speed, in contrast, produces separate vortex rings on both the downstroke and upstroke (Fig. 5A). Although representing the same fraction of peak labriform swimming speed in both species, 50 %$U_{p\text{-}c}$ corresponds to absolute swimming speeds that differ by a factor of 2 (Fig. 1). The single ring produced by the sunfish at 0.5 $L\,s^{-1}$ (approximately 10 $cm\,s^{-1}$) reflects a lower overall requirement for thrust production than that of the surfperch swimming at 1.0 $L\,s^{-1}$ (approximately 20 $cm\,s^{-1}$).

When the fishes swim at the same absolute speed, however, interspecific differences in wake structure are still observed. At 1.0 $L\,s^{-1}$, for example, both species generate measurable vorticity during the upstroke as well as the downstroke, but the wakes differ in the degree of development of the upstroke vortex filament. On the basis of vortex patterns observed in the frontal plane, Drucker and Lauder (1999) proposed that, at the end of the upstroke in sunfish, the developing upstroke vortex ring is not fully closed upon itself and instead terminates on

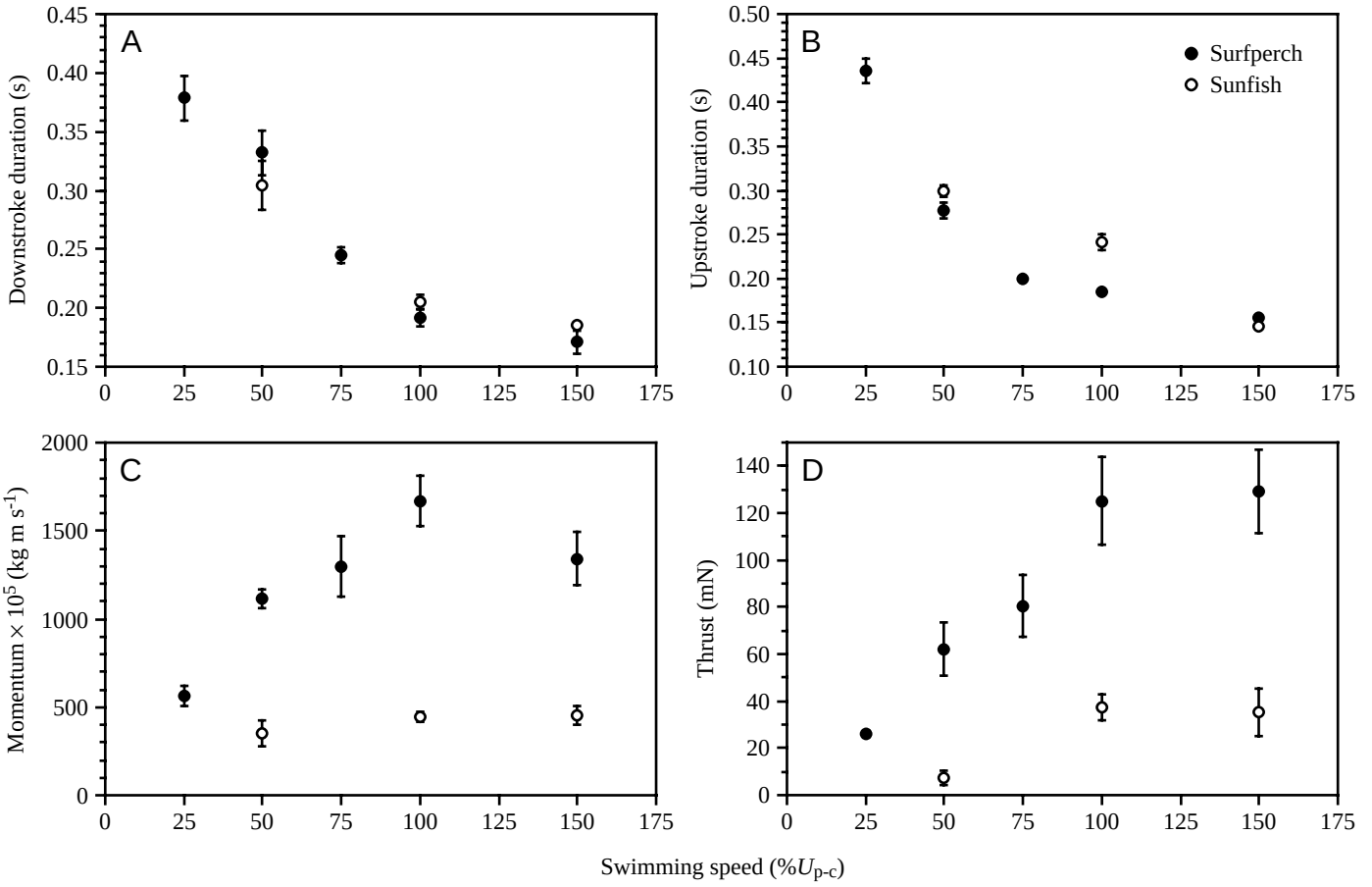

Fig. 7. Effects of swimming speed on fin stroke timing and wake variables in surfperch and sunfish. Data are plotted as means ± S.E.M. (N=3–6 fin strokes). Note that, for some plotted points, the error bars are obscured by the symbol. (A,B) Duration of pectoral fin half-strokes. (C) Summed momentum of downstroke and upstroke vortex rings, per fin. (D) Average forward thrust generated by both pectoral fins together over the course of a stride period. Statistical comparisons between the species (unpaired t-tests, d.f.=7–9) revealed significant differences at P=0.05 in the duration of the upstroke at 100 %$U_{p\text{-}c}$ (B) and in both momentum and thrust at all speeds studied (C,D). We propose that interspecific variation in stroke timing and wake momentum underlies the observed difference in thrust production of the two species. Sunfish data are from Drucker and Lauder (1999). $U_{p\text{-}c}$, pectoral–caudal gait transition speed.

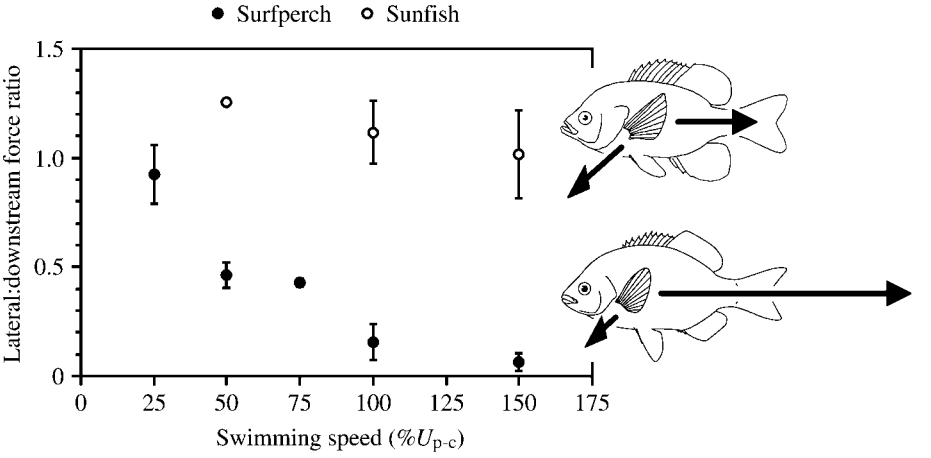

Fig. 8. Ratio of laterally to downstream-directed components of force (mean per stride ± S.E.M., N=3–10 fin strokes) for black surfperch and bluegill sunfish plotted as a function of swimming speed. In the surfperch, this ratio drops by a factor of more than 10 over the range of swimming speeds studied, while in the sunfish it declines only by a factor of 0.25, remaining near unity. The vectors accompanying the drawing of each fish represent the relative magnitudes of downstream and lateral force applied by the pectoral fins to the water at 150 %$U_{p\text{-}c}$ and, accordingly, of the thrust and inward-directed force experienced in reaction. These vectors are comparable both within and between species. See text for discussion. For two plotted points, the error bars fall within the dimensions of the symbol. $U_{p\text{-}c}$, pectoral–caudal gait transition speed.

the side of the body (Fig. 5E). At the same absolute speed, surfperch shed two complete and distinct vortex rings into the wake (Fig. 5A). The same interspecific pattern is observed when comparisons are made at constant fractions of the gait transition speed (Fig. 5B,E and C,F).

A further difference in wake geometry exhibited by the two species relates to the orientation of the central momentum jet of each vortex ring. In the surfperch, the downstroke ring faces ventrally and bears a fluid jet with a strong downward component of velocity. On the upstroke, the ring is tilted dorsally and the jet is oriented upwards (Figs 2B, 5A–C). The positive and negative lift forces that result from each half-stroke (Table 2), together with lift arising from the profile of the fish's body, must on average cancel over the course of many fin stroke cycles since the fish were not observed to follow a rising or sinking trajectory during labriform swimming. The dorsoventral orientation of the wake's momentum flow, however, suggests an imbalance of vertical forces acting on the surfperch at any particular moment during the stride. Such an imbalance can explain the dorsoventral surging or 'bobbing' that is observed in surfperches and other fast labroid fishes (Webb, 1973; Westneat, 1996; Walker and Westneat, 1997). Bobbing is negligible in slower pectoral fin swimmers such as sunfish (Gibb et al., 1994), an observation consistent with the production of vortex rings that are more upright in orientation (Fig. 5D–F).

Interspecific comparison of swimming forces

The total pectoral fin thrust and lift per stride calculated from DPIV data were partitioned into forces arising separately on the downstroke and upstroke (Table 2) to evaluate the relative contributions of each half-stroke to locomotor force. At most swimming speeds examined, both species exhibit an asymmetry in average force developed during the downstroke and upstroke. At low swimming speed ($0.5\,L\,s^{-1}$), the downstroke of the surfperch on average accounts for 41 % of the total thrust and 56 % of the total lift produced during the course of each complete fin stroke cycle. The balance (59 % and 44 % respectively) is created by the upstroke. At higher speeds, the importance of the downstroke increases: the ratio of downstroke force to total force peaks at 71 % for thrust and 79 % for lift at $U_{p\text{-}c}$, and above this speed declines (Table 2). In the sunfish, vortex rings and associated force are produced only during the downstroke at $0.5\,L\,s^{-1}$ (Fig. 5D). At higher speeds, the contribution of the upstroke grows, but does not exceed 27 % of total lift on average (Table 2, $1.5\,L\,s^{-1}$) and accounts for the majority (64 %) of total thrust only at the gait transition speed (Table 2, $1.0\,L\,s^{-1}$). Thus, in both species, the downstroke is the primary thrust- and lift-producing portion of the pectoral fin beat at most labriform swimming speeds. At swimming speeds representing comparable levels of exercise in the two species (100 and 150 %$U_{p\text{-}c}$; see Fig. 1), the downstroke thrust of the surfperch, measured as a proportion of total thrust, exceeds that of the sunfish by 1.2- to twofold. Absolute lift forces at these speeds are also substantially greater in the faster swimmer, but the sunfish generates a larger fraction of total lift with each downstroke than does the surfperch at the same percentages of $U_{p\text{-}c}$ (Table 2).

The mean thrust per stride generated by the pectoral fins at

Table 2. *Time-averaged thrust and lift forces calculated from the downstroke and upstroke wakes of black surfperch and bluegill sunfish*

		Surfperch						Sunfish					
		Thrust			Lift			Thrust			Lift		
Swimming speed	Stroke	Force	Total	Ratio	Force	Total	Ratio	Force	Total	Ratio	Force	Total	Ratio
$0.5\,L\,s^{-1}$	D	10.7			4.5			11.1			3.2		
	U	15.5	26.2	0.41	–3.5	8.0	0.56	–	11.1	1.00	–	3.2	1.00
$1.0\,L\,s^{-1}$	D	38.0			14.3			13.4			4.7		
	U	35.8	73.8	0.51	–6.9	21.2	0.67	24.2	37.6	0.36	–0.2	4.9	0.96
$1.5\,L\,s^{-1}$	D	56.5			35.6			19.1			16.0		
	U	24.0	80.5	0.70	–11.9	47.5	0.75	16.3	35.4	0.54	–5.9	21.9	0.73
$2.0\,L\,s^{-1}$	D	92.5			86.6								
	U	38.4	130.9	0.71	–23.3	109.9	0.79	–	–	–	–	–	–
$3.0\,L\,s^{-1}$	D	78.3			40.8								
	U	48.7	127.0	0.62	–39.9	80.7	0.51	–	–	–	–	–	–

Mean forces per stride (in mN) generated by both pectoral fins together are calculated at each speed from 3–8 fin strokes performed by two individuals of each species.

D, downstroke; U, upstroke; Total, sum of the absolute value of each half-stroke's force; Ratio, downstroke force expressed as a proportion of total force developed.

Positive and negative values of lift indicate upward and downward forces, respectively.

Data for sunfish are from Drucker and Lauder (1999).

L, total body length.

speeds up to $U_{p\text{-}c}$ (Fig. 7D) is assumed to be the total thrust generated by the fish to overcome drag. The steady-state expectation for the drag D acting on a streamlined body, such as that of a fish, is given by:

$$D = \tfrac{1}{2}\rho U^2 A C_D, \quad (2)$$

where ρ is the density of water, U is the forward swimming speed, A is the projected area of the body and C_D is the drag coefficient (Vogel, 1994). The drag acting on the oscillating pectoral fins, however, changes dynamically and is proportional to the second power of the velocity of incident flow, which is influenced both by U and by the fin flapping velocity (cf. Ellington, 1984), which changes unsteadily over time. Thus, the total average drag per stroke cycle on a fish swimming with the pectoral fins will not necessarily follow the quadratic relationship to speed given in equation 2. In *Embiotoca jacksoni* and *Lepomis macrochirus*, the time-averaged pectoral fin thrust per stride indeed increases linearly with U up to $U_{p\text{-}c}$ (Fig. 7D). For both species, the incremental rate of increase in thrust with speed is approximately 60 mN per $L\,s^{-1}$. The absence of an obvious quadratic relationship between thrust and swimming speed for the species studied may be a result of (i) possible effects of the mucus coating of the body and fins acting to diminish the rate of increase in total drag with speed (Hoyt, 1975; Bernadsky et al., 1993), (ii) the narrow range of absolute swimming speeds over which thrust data were collected (note, however, that we examined the biologically relevant range of labriform swimming speeds in these species), or (iii) the reduction in drag that occurs as the boundary layer makes its transition from laminar to turbulent flow with increasing speed. The Reynolds number for the fish studied here (calculated using total body length) varies from 2.1×10^4 to 1.2×10^5, a range in which flow around streamlined bodies indeed becomes transitional and drag forces do not rise quadratically with increasing speed (Shapiro, 1961; Vogel, 1994). Changing boundary-layer flow conditions over the range of speeds examined in the present study may therefore result in a lower rate of increase in drag (and hence thrust) than would be expected at higher speeds above the transition to a turbulent boundary layer.

The black surfperch and bluegill sunfish differ by a factor of 3–4 in the total pectoral fin thrust that is generated at the upper limit of the labriform swimming gait (Fig. 7D). What hydrodynamic or kinematic features of the fin beat might explain this difference? Thrust is related both to the momentum of the vortex wake and to the period of propulsor movement, during which momentum is added to the fluid (equation 1). The only significant interspecific difference in fin stroke timing was observed at the pectoral–caudal gait transition speed ($U_{p\text{-}c}$). At $U_{p\text{-}c}$, the surfperch exhibits a significantly faster upstroke than the sunfish (Fig. 7B), a difference that contributes to the surfperch's greater thrust at this speed (Fig. 7D). Differences in wake momentum, in contrast, were observed at all swimming speeds (Fig. 7C) and can account more completely for the higher forces developed by the surfperch.

Underlying this difference in momentum are two important differences in the structure of the animals' wakes. The appearance of no more than two vortices in frontal-plane transections of the wake of the sunfish (Fig. 5E,F, *F*1, *F*2) indicates that the upstroke vortex loop is not closed upon itself at the end of the upstroke. Vortex ring momentum is proportional to both mean vortex circulation Γ and ring area A (equation 3 in Drucker and Lauder, 1999). The downstroke and upstroke rings of sunfish do not differ significantly in Γ (unpaired *t*-tests at 1.0 and 1.5 $L\,s^{-1}$, d.f.=8,10; P=0.15, 0.82, Table 1). While the radii of these rings are also statistically indistinguishable (unpaired *t*-tests, d.f.=14,16; P=0.06, 0.37, Table 1), the upstroke loop is incomplete, thereby possessing lower area. With the assumption that unsteady hydrodynamic phenomena, such as the Wagner effect, have equal influence on Γ during each half-stroke (see Dickinson, 1996), the incomplete upstroke vortex loop (Fig. 5E,F) is therefore expected to add less momentum to the wake than would a complete loop. In the surfperch, in contrast, the production of four distinct frontal-plane vortices at all speeds (Fig. 5A–C, *F*1–*F*4) reflects the shedding of two complete vortex rings away from the body. At comparable swimming speeds, surfperch generate rings that are significantly larger and stronger than those produced by sunfish (unpaired *t*-tests at 50, 100 and 150 %$U_{p\text{-}c}$, d.f.=6–15, P<0.01). At fixed fractions of $U_{p\text{-}c}$, surfperch produce rings whose radius exceeds that of sunfish rings by as much as 1.6 cm and whose total vortex circulation (the sum of downstroke and upstroke Γ magnitude) surpasses that of sunfish by 8–43 $cm^2\,s^{-1}$ (Table 1). Augmenting A and Γ is a mechanism for imparting greater momentum to the wake (Fig. 7C).

A second relevant interspecific difference in wake geometry involves the orientation of the wake's central momentum jet. The average orientation of water velocity vectors interposed in the downstroke vortex pair changes markedly with swimming speed. In the frontal plane, downstroke jet angle ϕ in the surfperch decreases with speed, reaching nearly 0° on average at 150 %$U_{p\text{-}c}$ (Fig. 6), reflecting a largely downstream orientation of momentum flow and an increasing contribution of the paired fins to forward thrust. In spite of the immediate demand for thrust at high speeds, the sunfish increases ϕ to approximately 90° during the downstroke (Fig. 6), thereby exerting a relatively large lateral component of force. We propose that this difference in momentum jet orientation, together with the difference in vortex ring area and circulation discussed above, provides a hydrodynamic explanation for both the observed interspecific difference in thrust production and the variation between species in maximum labriform swimming speed.

Aside from differences in wake dynamics correlated with differences in thrust, there are in addition anatomical, neuromuscular and physiological variables that may help to explain the observed interspecific variation in $U_{p\text{-}c}$. Pectoral fin shape and kinematics have been proposed to influence swimming force in theoretical studies of labriform locomotion (Blake, 1979, 1981), and differences between the bluegill sunfish and black surfperch in pectoral fin form and motion

may indeed contribute to differences in maximum swimming speed. In addition, variation in pectoral fin muscle mass and physiology will lead to interspecific differences in thrust force and power. The mechanical properties of pectoral fin muscle have been described for sunfish (Luiker and Stevens, 1992, 1993) but not for surfperch; obtaining such measurements will be an important next step in understanding the physiological basis of differences in labriform swimming performance. Fishes capable of prolonged high-speed swimming have also been shown to possess a greater proportion of aerobic fibers in the locomotor muscle than slower-swimming fishes (Boddeke et al., 1959). Variation in the composition of fiber types within pectoral fin muscle might further contribute to an explanation for differences in maximum speed.

Both the analysis of the internal power output of locomotor muscle and the study of how such power is transmitted to the fluid are needed to understand fully the observed variation among species in maximum swimming speed. Without an analysis of interspecific differences in locomotor muscle physiology, we will not know the extent to which species differ in the amount of power that can be delivered to the fins. But without also an understanding of the hydrodynamic interactions between the propulsors and the fluid, we will be unable to predict how species differ in the efficiency of transformation of internal mechanical energy to external work on the environment. As an example, in bluegill sunfish, no change in fiber type composition or increase in the amount of power generated by the pectoral fin muscles will be sufficient to increase the downstroke's contribution to maximal swimming speed since the locomotor force at high speed is directed laterally, almost at right angles to the direction of movement (Fig. 6).

Stability and maneuverability

The production of large laterally oriented forces by both surfperch and sunfish at low swimming speeds and the maintenance of such large lateral forces in sunfish even at high speeds (Fig. 8) are remarkable and unexpected results of the analysis of the vortex wake. At the lowest speeds studied for each species, the laterally directed forces nearly equal (surfperch) or significantly exceed (sunfish) the thrust forces. These data suggest two hypotheses concerning stability and maneuverability during pectoral fin locomotion in these species. First, large lateral forces may be necessary for locomotor stability. In bluegill sunfish (comparable data are not available for surfperch), the center of buoyancy is located near the center of mass (Webb and Weihs, 1994), yet large laterally oriented forces may still be needed to stabilize the body during steady horizontal swimming. This hypothesis suggests that bluegill sunfish should be relatively resistant to mediolateral perturbations during pectoral fin swimming compared with black surfperch. Second, large lateral forces may be associated with increased maneuverability. The ability of a fish to change its heading by modulating the force balance between the left and right fins may be enhanced if the magnitude or direction of the force exerted by one fin is suddenly altered. Large laterally directed forces exerted by a fin on one side of the body will generate rapid body turning to the opposite side. This hypothesis predicts that bluegill sunfish should exhibit a turning performance superior to that of black surfperch, especially at speeds between 50 and 150 %$U_{p\text{-}c}$ (Fig. 8). An additional implication of this second hypothesis is that a hydrodynamic trade-off between speed and maneuverability may exist that emerges from the geometric orientation of vortex rings shed by the fins. When the vortex wake is oriented primarily laterally, thrust, of necessity, will be limited but the capacity for turning enhanced. Species that shed vortex rings oriented primarily posteriorly will exhibit elevated thrust production at the expense of laterally directed force generation. The ability of fishes to circumvent this trade-off may depend on the orientation and flexibility of the fin base, which should limit the ability to vary the direction of vortex ring shedding into the wake. The relationship between pectoral fin orientation, kinematic versatility and wake structure is a completely unexplored area that holds considerable promise for clarifying the hydrodynamic significance of pectoral fin morphology in fishes.

We thank J. Liao, J. Nauen, J. Posner and C. Wilga for helpful discussions and two anonymous reviewers for valuable comments on the manuscript. Animals were kindly supplied by Mark Akins, Shane Anderson and Ted Mainey. Supported by NSF DBI-9750321 to E.G.D. and NSF IBN-9807012 to G.V.L.

References

Bernadsky, G., Sar, N. and Rosenberg, E. (1993). Drag reduction of fish skin mucus: relationship to mode of swimming and size. *J. Fish Biol.* **42**, 797–800.

Blake, R. W. (1979). The mechanics of labriform locomotion. I. Labriform locomotion in the angelfish (*Pterophyllum eimekei*): an analysis of the power stroke. *J. Exp. Biol.* **82**, 255–271.

Blake, R. W. (1981). Influence of pectoral fin shape on thrust and drag in labriform locomotion. *J. Zool., Lond.* **194**, 53–66.

Boddeke, R., Slijper, E. J. and Stelt, A. V. D. (1959). Histological characteristics of the body-musculature of fishes in connection with their mode of life. *Proc. K. Ned. Akad. Wet.* **62**, 576–588.

Bray, R. N. and Ebeling, A. W. (1975). Food, activity, and habitat of three 'picker-type' microcarnivorous fishes in the kelp forests off Santa Barbara, California. *Fish. Bull.* **73**, 815–829.

Brodsky, A. K. (1991). Vortex formation in the tethered flight of the peacock butterfly *Inachis io* L. (Lepidoptera, Nymphalidae) and some aspects of insect flight evolution. *J. Exp. Biol.* **161**, 77–95.

Carrier, D., Gregersen, C. and Silverton, N. (1998). Dynamic gearing in running dogs. *J. Exp. Biol.* **201**, 3185–3195.

DeMartini, E. E. (1969). A correlative study of the ecology and comparative feeding mechanism morphology of the Embiotocidae (surf-fishes) as evidence of the family's adaptive radiation into available ecological niches. *Wasmann J. Biol.* **27**, 177–247.

Dickinson, M. H. (1996). Unsteady mechanisms of force generation in aquatic and aerial locomotion. *Am. Zool.* **36**, 537–554.

Drucker, E. G. (1996). The use of gait transition speed in comparative studies of fish locomotion. *Am. Zool.* **36**, 555–566.

Drucker, E. G. and Lauder, G. V. (1999). Locomotor forces on a

swimming fish: three-dimensional vortex wake dynamics quantified using digital particle image velocimetry. *J. Exp. Biol.* **202**, 2393–2412.

Ebeling, A. W., Larson, R. J., Alevizon, W. S. and Bray, R. N. (1980). Annual variability of reef-fish assemblages in kelp forests off Santa Barbara, California. *Fish. Bull.* **78**, 361–377.

Ellington, C. P. (1984). The aerodynamics of hovering insect flight. IV. Aerodynamic mechanisms. *Phil. Trans. R. Soc. Lond. B* **305**, 79–113.

Gibb, A. C., Jayne, B. C. and Lauder, G. V. (1994). Kinematics of pectoral fin locomotion in the bluegill sunfish *Lepomis macrochirus*. *J. Exp. Biol.* **189**, 133–161.

Hixon, M. A. (1980). Competitive interactions between California reef fishes of the genus *Embiotoca*. *Ecology* **61**, 918–931.

Hoyt, J. W. (1975). Hydrodynamic drag reduction due to fish slimes. In *Swimming and Flying in Nature*, vol. 2 (ed. T. Wu, C. Brokaw and C. Brennen), pp. 653–672. New York: Plenum Press.

Jensen, J. S. (1993). Relationships and trophic functional morphology of the Embiotocidae (Perciformes). PhD dissertation, Harvard University.

Keast, A. and Webb, D. (1966). Mouth and body form relative to feeding ecology in the fish fauna of a small lake, Lake Opinicon, Ontario. *J. Fish. Res. Bd Can.* **23**, 1845–1874.

Lauder, G. V. (2000). Function of the caudal fin during locomotion in fishes: kinematics, flow visualization and evolutionary patterns. *Am. Zool.* **40**, 101–122.

Luiker, E. A. and Stevens, E. D. (1992). Effect of stimulus frequency and duty cycle on force and work in fish muscle. *Can. J. Zool.* **70**, 1135–1139.

Luiker, E. A. and Stevens, E. D. (1993). Effect of stimulus train duration and cycle frequency on the capacity to do work in pectoral fin muscle of the pumpkinseed sunfish, *Lepomis gibbosus*. *Can. J. Zool.* **71**, 2185–2189.

Maxworthy, T. (1972). The structure and stability of vortex rings. *J. Fluid Mech.* **51**, 15–32.

Milne-Thomson, L. M. (1966). *Theoretical Aerodynamics*, 4th edition. New York: Macmillan.

Raffel, M., Willert, C. E. and Kompenhans, J. (1998). *Particle Image Velocimetry: A Practical Guide*. Heidelberg: Springer-Verlag.

Rayner, J. M. V., Jones, G. and Thomas, A. (1986). Vortex flow visualizations reveal change in upstroke function with flight speed in bats. *Nature* **321**, 162–164.

Roberts, T., Kram, R., Weyand, P. and Taylor, C. R. (1998). Energetics of bipedal running. I. Metabolic cost of generating force. *J. Exp. Biol.* **201**, 2745–2751.

Rome, L. C., Funke, R. P., Alexander, R. McN., Lutz, G., Aldridge, H., Scott, F. and Freadman, M. (1988). Why animals have different muscle fibre types. *Nature* **335**, 824–827.

Rome, L. C., Sosnicki, A. and Choi, I. (1992). The influence of temperature on muscle function in the fast swimming scup. II. The mechanics of red muscle. *J. Exp. Biol.* **163**, 281–295.

Shapiro, A. H. (1961). *Shape and Flow: The Fluid Dynamics of Drag*. New York: Doubleday & Co.

Spedding, G. R. (1986). The wake of a jackdaw (*Corvus monedula*) in slow flight. *J. Exp. Biol.* **125**, 287–307.

Spedding, G. R., Rayner, J. M. V. and Pennycuick, C. J. (1984). Momentum and energy in the wake of a pigeon (*Columba livia*) in slow flight. *J. Exp. Biol.* **111**, 81–102.

Vogel, S. (1994). *Life in Moving Fluids: The Physical Biology of Flow*, 2nd edition. Princeton: Princeton University Press.

Walker, J. A. and Westneat, M. W. (1997). Labriform propulsion in fishes: kinematics of flapping aquatic flight in the bird wrasse *Gomphosus varius* (Labridae). *J. Exp. Biol.* **200**, 1549–1569.

Wardle, C. S. (1975). Limits of fish swimming speed. *Nature* **255**, 725–727.

Wardle, C. S. and Videler, J. J. (1979). How do fish break the speed limit? *Nature* **284**, 445–447.

Webb, P. W. (1973). Kinematics of pectoral fin propulsion in *Cymatogaster aggregata*. *J. Exp. Biol.* **59**, 697–710.

Webb, P. W. and Weihs, D. (1994). Hydrostatic stability of fish with swim bladders: not all fish are unstable. *Can. J. Zool.* **72**, 1149–1154.

Werner, E. E. and Hall, D. J. (1974). Optimal foraging and size selection of prey by the bluegill sunfish (*Lepomis macrochirus*). *Ecology* **55**, 1042–1052.

Westneat, M. W. (1996). Functional morphology of aquatic flight in fishes: kinematics, electromyography, and mechanical modeling of labriform locomotion. *Am. Zool.* **36**, 582–598.

Wilga, C. D. and Lauder, G. V. (1999). Locomotion in sturgeon: function of the pectoral fins. *J. Exp. Biol.* **202**, 2413–2432.